RSC Advances

ROYAL SOCIETY
OF CHEMISTRY

www.rsc.org/advances

Journal Name

COMMUNICATION

Synthesis of core-shell structured Fe₃O₄@α-MnO₂ microspheres for efficiently catalytic degradation of ciprofloxacin

Huan Zhao, Hao-Jie Cui[*] and Ming-Lai Fu[*]

Three-dimensional core-shell structured Fe₃O₄@α-MnO₂ microspheres were successfully fabricated by two-step hydrothermal method. The obtained magnetic microspheres exhibit excellent ability to activate persulfate for catalytic degradation of ciprofloxacin in wastewater with easy magnetic separation.

Ciprofloxacin (CIP), as an important fluoroquinolone antibiotic, has been extensively used for treatment of both human and animal diseases. CIP residues may enter environments through wastewater effluents, which could lead to the development of antibiotic resistant bacteria and potential risks to human health.[1-3] Therefore, developing effective methods to remove CIP from polluted water has attracted intensive attentions in the recent years.[4-7]

In the past years, sulfate radical (SO₄•⁻) based advanced oxidation technologies have become a hotspot due to its high efficiency for mineralization of organic pollutants.[8] It has been proved that the persulfate (PS) can be activated by UV,[9] heat,[10] base,[11] transition metal ions,[12, 13] and metal oxides to generate SO₄•⁻.[14-16] Among these activation methods, UV, heat and base activation intensively consume energy or chemicals, and the use of transition metal ions for activating PS is limited in a narrow pH range (acid medium). Recently, manganese oxides received particular attention to heterogeneously activate PS due to their excellent catalytic activity and low toxicity.[17-19] However, the effective approaches for catalysts recovery is a bottleneck for their practical application. Thus, developing novel and recoverable metal oxide catalysts to activate PS for CIP degradation in wastewater is of great interest. In our previous work, magnetic iron oxides containing manganese (MnFe₂O₄ and Mn doped α-Fe₂O₃) have been successfully synthesized as adsorbents to remove heavy metal ions and organic dyes with higher capacities and easy magnetic separation.[20, 21] However, these magnetic nanomaterials containing Mn showed poor performance to activate PS, taking into account the excellent catalytic activity of manganese oxides for activating PS , we extend our research on the fabrication of expected magnetic manganese oxides as an effective catalyst to activate PS for removal of CIP.

Herein, α-MnO₂, which has been proved to be of higher catalytic activity than other manganese oxides for activation of PS,[18] was successfully coated on Fe₃O₄ microspheres as nanosheets by hydrothermal method. As expected, the synthesized core-shell structured Fe₃O₄/α-MnO₂ microspheres exhibit excellent ability in activation of PS to generate SO₄•⁻ for CIP degradation, and the catalysts were feasible for the fast recyclable treatment via simple magnetic separation. To the best of our knowledge, this kind of magnetic core-shell structured Fe₃O₄/α-MnO₂ microspheres has not been reported before. This material could be used as catalysts for effectively removing organic pollutants from wastewater.

Fig. 1a showed the typical XRD patterns of the bare Fe₃O₄ and Fe₃O₄@α-MnO₂ microspheres. All the detected diffraction peaks in the pattern of Fe₃O₄ can be assigned to magnetite (JCPDS No. 75-1609).[22] After coating with manganese oxide, an extra characteristic diffraction peak at 12.80° was detected in the pattern of Fe₃O₄@α-MnO₂ microspheres, which can be indexed as (110) diffractions of α-MnO₂ (JCPDS No. 44-0141).[23] The morphologies and structures of the as-synthesized products were further investigated by SEM and TEM. Fig. S1 showed the SEM image of the Fe₃O₄ microspheres and it can be seen that the products have a relatively uniform diameter of 300-400 nm. A general overview of the Fe₃O₄@α-
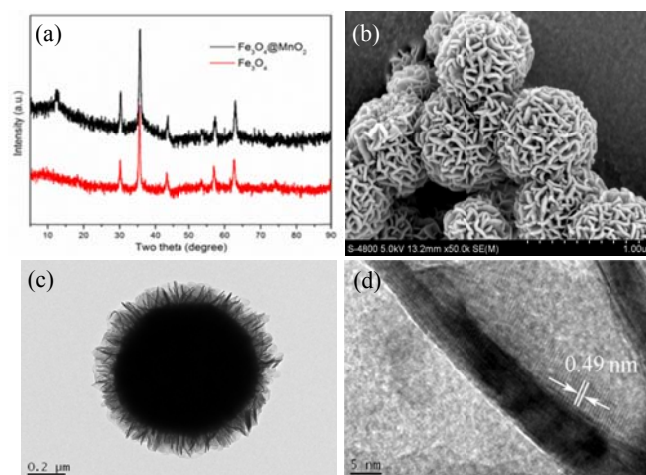
Fig. 1 XRD patterns of Fe₃O₄ and the synthesized Fe₃O₄@α-MnO₂ microspheres (a), SEM (b) and TEM (c and d) images of the synthesized Fe₃O₄@α-MnO₂ microspheres.
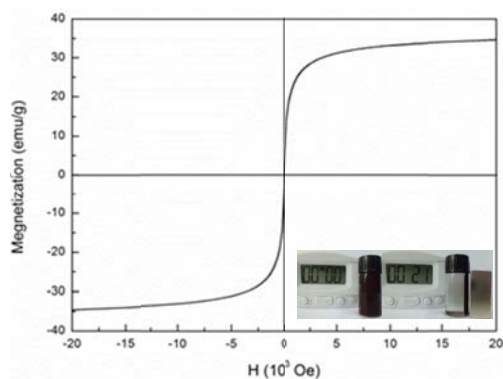
Fig. 2 The magnetization hysteresis of the as-synthesized $Fe_3O_4@\alpha\text{-}MnO_2$ microspheres.

MnO_2 microspheres was shown in Fig. 1b, which indicated that the Fe_3O_4 microspheres were fully decorated with uniform manganese oxide nanosheets and all the wrapped microspheres have three-dimensional flowerlike hierarchical morphology with a diameter of 500-600 nm. Fig. 1c illustrates the TEM image of $Fe_3O_4@\alpha\text{-}MnO_2$, in which the dark regions represented the Fe_3O_4 microsphere and the bright regions represented the $\alpha\text{-}MnO_2$ shell. It was clearly displayed that the Fe_3O_4 core was well wrapped by the $\alpha\text{-}MnO_2$ nanosheets, and the average thickness of the $\alpha\text{-}MnO_2$ coating shell was about 100 nm. HRTEM observations demonstrated that the $\alpha\text{-}MnO_2$ nanosheets were with a thickness of about 5 nm (Fig. 1d). Moreover, the lattice fringes were clearly visible with a spacing of 0.49 nm, which was in good agreement with the spacing of the (200) planes of $\alpha\text{-}MnO_2$.[24] The EDX spectrum of the $Fe_3O_4@\alpha\text{-}MnO_2$ microspheres confirms the presence of Mn, Fe and O elements (Fig. S2), validating the purity of the material. The above results indicated that the Fe_3O_4 core can be well wrapped by $\alpha\text{-}MnO_2$ nanosheets coating layer through a simple hydrothermal deposition method.

Magnetization curve was measured for the core-shell structured $Fe_3O_4@\alpha\text{-}MnO_2$ microspheres at room temperature. As depicted in Fig. 2, it was hardly to see an obvious hysteresis loop at the full scale for the composites, indicating the superparamagnetism of the core-shell structured $Fe_3O_4@\alpha\text{-}MnO_2$ microspheres. It can be obtained from Fig. 2 that the magnetization saturation value was about 34.6 emu g^{-1} for the $Fe_3O_4@\alpha\text{-}MnO_2$ microspheres. The magnetization value was lower than that of the pure Fe_3O_4 microspheres.[22] Such decrease might be due to the loading of $\alpha\text{-}MnO_2$ on the Fe_3O_4 microspheres. Despite the reduction in magnetic strength, the
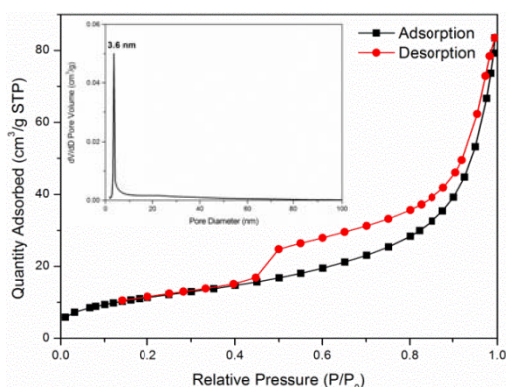
Fig. 3 N_2 adsorption/desorption isotherms and pore size distributions of the as-synthesized $Fe_3O_4@\alpha\text{-}MnO_2$ microspheres.
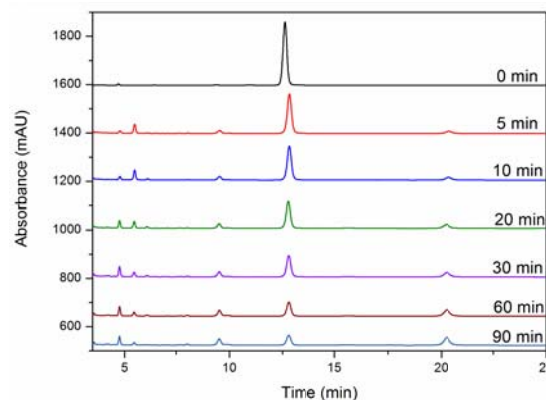

Fig. 4 HPLC chromatograms of a solution of CIP (50 mg L^{-1}) in the presence of $Fe_3O_4@\alpha\text{-}MnO_2$ microspheres (1 g L^{-1}) and $Na_2S_2O_8$ (2 g L^{-1}) treated at 25 °C for different time intervals.

materials were still strongly magnetic and enable magnetic manipulation and recovery of the catalyst in the water treatment, as shown in inset in Fig. 2.

In order to examine the pore characteristic of the core-shell structured $Fe_3O_4@\alpha\text{-}MnO_2$ microspheres, Brunnauer-Emmett-Teller (BET) N_2 adsorption/desorption measurements were performed. The isothermal plots of N_2 adsorption/desorption for the $Fe_3O_4@\alpha\text{-}MnO_2$ microspheres showed type IV isotherms, which indicated monolayer adsorption at low pressure and multilayer adsorption at high pressure, and showed fairly hysteresis loop between adsorption and desorption in the P/P_0 range above 0.4, indicating a mesoporous structure, as illustrated in Fig. 3. Based on the BET equation, the specific surface area of the $Fe_3O_4@\alpha\text{-}MnO_2$ microspheres was 42.0 m^2 g^{-1}, which is higher than that of pure Fe_3O_4 microspheres (30.9 m^2 g^{-1}) and $\alpha\text{-}MnO_2$ (29.6 m^2 g^{-1}) (Fig. S3). The pore size distribution of the composites, calculated from desorption data using Barett-Joyner-Halenda (BJH) model, showed one narrow peak centered at ~3.6 nm (insert in Fig. 3).

The synthesized $Fe_3O_4@\alpha\text{-}MnO_2$ microspheres were tested for their catalytic performance in the oxidation of CIP as a model with PS under controlled conditions (Fig. 4). The spectrum at $t = 0$ was obtained for a starting solution of CIP with a concentration of 50 mg L^{-1} (without catalyst and PS), and only one characteristic absorption peak (12.8 min) of the CIP could be observed in the HPLC chromatogram. As soon as $Fe_3O_4@\alpha\text{-}MnO_2$ microspheres and PS were added, the intensities of the peak slightly decreased after a 5-min reaction, and four relative peaks of the intermediates were detected, indicating that a little amount of CIP were degraded during initial catalytic degradation. As the reaction time elapsed, the CIP peak continued to drop at a slower rate. Within 90 min, the characteristic absorption band of CIP became broader and weaker, suggesting that most of CIP were degraded.

The degree of degradation was expressed as $(I_0\text{-}I)/I_0$, where I_0 is the absorption at $t = 0$ and I is the absorption at a given reaction time. Fig. 5 showed CIP removal in PS and $Fe_3O_4@\alpha\text{-}MnO_2$ solution alone, and PS coupled with Fe_3O_4 microspheres, $Fe_3O_4@\alpha\text{-}MnO_2$ microspheres, and $\alpha\text{-}MnO_2$. It was observed that the addition of PS in the absence of any catalyst brought
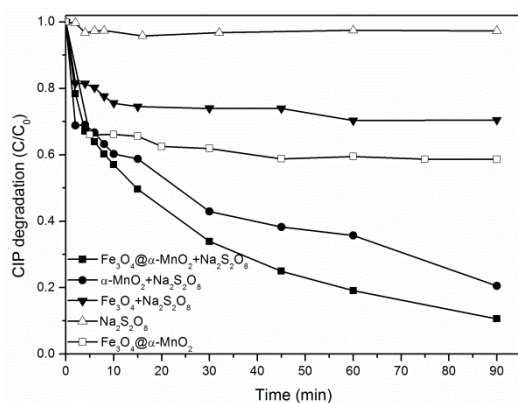
Fig. 5 Ciprofloxacin degradation profiles versus time in different systems (initial CIP concentration 50 mg L^{-1}, $Na_2S_2O_8$ concentration 2 g L^{-1}, catalyst load 1 g L^{-1}).

about 3% of CIP removal in 90 min, and the addition of $Fe_3O_4@\alpha-MnO_2$ alone enhanced the CIP degradation and the removal of CIP was 41.4%, which could be attributed to adsorption of CIP on the $Fe_3O_4@\alpha-MnO_2$ microspheres. The simultaneous use of $Fe_3O_4@\alpha-MnO_2$ and PS promoted the CIP degradation significantly, yielding a CIP removal of 90% in 90 min, which was higher than the CIP removal of 79.5% and 29.5%, achieved by adding $\alpha-MnO_2$ and Fe_3O_4 as the catalyst, respectively. These results indicated that the core-shell structured $Fe_3O_4@\alpha-MnO_2$ microspheres could enhance the catalytic degradation of CIP in the present of PS. The TOC concentration of the solution decreased from 28.5 mg L^{-1} of the initial solution to 16.5 mg L^{-1} of reacted solution, indicating that some of the CIP has not been degraded completely after reaction for 90 min. It should be noted that the CIP could be mineralized completely by prolonging reaction time.

Sulfate radical has been proposed to be the actual oxidant species in activated PS processes. However, hydroxyl radical can also be generated due to the reaction of $SO_4^{\bullet-}$ with H_2O.[12, 16] The nascent free radical species have high oxidizing ability for oxidation of the CIP. To identify the catalytic role of the potential species, ethanol (EtOH) and *tert*-butanol (TBA) scavenger, which have different reaction rate constants with sulfate radical and hydroxyl radical, were added to the catalytic system.[16] In the presence of EtOH, the degradation of CIP obviously decreased (Fig. S4). In contrast, the presence of TBA has slight effect on CIP degradation. These results suggested that sulfate radical was the main oxidant species responsible for CIP degradation in the magnetic composites/PS coupled process. Moreover, the prepared core-shell structured $Fe_3O_4/\alpha-MnO_2$ microspheres showed superior stability during the activated PS reaction, and more than 85% of the CIP could be decomposed after duplicating the catalytic reaction 5 times (Fig. S5). The above observations indicated that the as-synthesized core-shell structured $Fe_3O_4/\alpha-MnO_2$ microspheres could be used as a potential catalyst for organic pollutants degradation.

Conclusions

In summary, three-dimensional core-shell structured $Fe_3O_4/\alpha-MnO_2$ microspheres have been successfully synthesized by two-step hydrothermal method. The crystal $\alpha-MnO_2$ loaded on the Fe_3O_4 microspheres as nanosheets with thickness of about 5 nm. The obtained products showed high ability to activate PS

for degradation of CIP from the solution with easy magnetic separation. These results implied that this material could be used as catalyst for effectively degradation of organic pollutants from wastewater.

Notes and references

Institute of Urban Environment, Chinese Academy of Sciences, Xiamen 361021, China. E-mail: hjcui@iue.ac.cn; mlfu@iue.ac.cn.

† Electronic Supplementary Information (ESI) available: Detail experimental procedures, SEM image of the Fe_3O_4 microspheres, EDX spectrum of the composites, N_2 adsorption/desorption isotherms of the pure Fe_3O_4 microspheres and $\alpha-MnO_2$, degradation of CIP in the system of PS/$Fe_3O_4@\alpha-MnO_2$ without and with quenching agents of TBA (0.10 mol L^{-1}) and EtOH (0.10 mol L^{-1}), and time profiles of CIP degradation in different recycles. See DOI: 10.1039/c000000x/

1. J. L. Martínez, *Science*, 2008, **321**, 365.
2. Q. Zhang, G. Lambert, D. Liao, H. Kim, K. Robin, C.-k. Tung, N. Pourmand and R. H. Austin, *Science*, 2011, **333**, 1764.
3. I. Michael, L. Rizzo, C. S. McArdell, C. M. Manaia, C. Merlin, T. Schwartz, C. Dagot and D. Fatta-Kassinos, *Water Res.*, 2013, **47**, 957.
4. B. DeWitte, J. Dewulf, K. Demeestere, V. Van De Vyvere, P. De Wispelaere and H. Van Langenhove, *Environ. Sci. Technol.*, 2008, **42**, 4889.
5. T. Paul, M. C. Dodd and T. J. Strathmann, *Water Res.*, 2010, **44**, 3121.
6. S. A. C. Carabineiro, T. Thavorn-Amornsri, M. F. R. Pereira and J. L. Figueiredo, *Water Res.*, 2011, **45**, 4583.
7. S. P. Sun, T. A. Hatton and T.-S. Chung, *Environ. Sci. Technol.*, 2011, **45**, 4003.
8. I. Hussain, Y. Zhang and S. Huang, *RSC Adv.*, 2014, **4**, 3502.
9. J.-Y. Fang and C. Shang, *Environ. Sci. Technol.*, 2012, **46**, 8976.
10. R. L. Johnson, P. G. Tratnyek and R. O. B. Johnson, *Envirn. Sci. Technol.*, 2008, **42**, 9350-9356.
11. O. S. Furman, A. L. Teel and R. J. Watts, *Environ. Sci. Technol.*, 2010, **44**, 6423.
12. G. P. Anipsitakis and D. D. Dionysiou, *Envirn. Sci. Technol.*, 2004, **38**, 3705.
13. J. Zou, J. Ma, L. Chen, X. Li, Y. Guan, P. Xie and C. Pan, *Envirn. Sci. Technol.*, 2013, **47**, 11685.
14. G.-D. Fang, D. D. Dionysiou, S. R. Al-Abed and D.-M. Zhou, *Appl. Catal. B: Environ.*, 2013, **129**, 325.
15. T. Zhang, H. Zhu and J.-P. Croué, *Envirn. Sci. Technol.*, 2013, **47**, 2784.
16. Y. Ding, L. Zhu, N. Wang and H. Tang, *Appl. Catal. B: Environ.*, 2013, **129**, 153.

17. Y. Yao, C. Xu, S. Yu, D. Zhang and S. Wang, *Ind. Eng. Chem. Res.*, 2013, **52**, 3637.

18. E. Saputra, S. Muhammad, H. Sun, H. M. Ang, M. O. Tadé and S. Wang, *Envirn. Sci. Technol.,* 2013, **47**, 5882.

19. E. Saputra, S. Muhammad, H. Sun, H.-M. Ang, M. O. Tadé and S. Wang, *Appl. Catal. B: Environ.*, 2014, **154–155**, 246.

20. H.-J. Cui, J.-K. Cai, J.-W. Shi, B. Yuan, C.-L. Ai and M.-L. Fu, *RSC Adv.*, 2014, **4**, 10176.

21. H.-J. Cui, J.-W. Shi, B. Yuan and M.-L. Fu, *J. Mater. Chem. A*, 2013, **1**, 5902.

22. H. Deng, X. Li, Q. Peng, X. Wang, J. Chen and Y. Li, *Angew. Chem.*, 2005, **117**, 2842.

23. D. Su, H.-J. Ahn and G. Wang, *J. Mater. Chem. A*, 2013, **1**, 4845.

24. D. Yu, J. Yao, L. Qiu, Y. Wang, X. Zhang, Y. Feng and H. Wang, *J. Mater. Chem. A*, 2014, **2**, 8465.